Utilization of Zinc-Ferrite/ Water Hybrid Nanofluids for enhancing thermal performance of a Flat Plate Solar Collector -An Analytical Study

Prakasam Michael Joseph stalin (pmjstalin@gmail.com)
ASCET: Audisankara College of Engineering and Technology
Thottipalayam Vellingri Arjunan
Guru Ghasidas Vishwavidyalaya: Guru Ghasidas University
Mohammed Abdulrahman Almeshaal
Imam Muhammad bin Saud Islamic University: Imam Muhammad Ibn Saud Islamic University
Palaniappan Murugesan
Imam Muhammad Ibn Saud Islamic University
Balaramachandran Prabu
Christian College of Engineering
Pasupathi Manoj Kumar
KPR Institute of Engineering and Technology

Research Article

Keywords: Solar collector, Hybrid Nanofluid, Zinc-ferrite/Water, Thermal performance, Exergy

Posted Date: November 15th, 2021

DOI: https://doi.org/10.21203/rs.3.rs-976278/v1

Utilization of Zinc-Ferrite/ Water Hybrid Nanofluids for enhancing thermal performance of a Flat Plate Solar Collector -An Analytical Study

Prakasam Michael Joseph Stalin[1]*, Thottipalayam Vellingri Arjunan[2], Mohammed Abdulrahman Almeshaal[3], Palaniappan Murugesan[4], Balaramachandran Prabu[5], Pasupathi Manoj Kumar[6]

[1]Audisankara College Engineering &Technology, Gudur-524101, India.

[2] Guru GhasidasViswavidyalaya (Central University), Chhattisgarh -495009, India.

[3,4]Imam Mohammad Ibn Saud Islamic University, Riyadh - 11432, Saudi Arabia

[5]Christian College of Engineering and Technology, Oddanchatram.- 624619, India.

[6]KPR Institute of Engineering and Technology, Coimbatore-641407, India.

* Corresponding Author: Email: -pmjstalin@gmail.com, 9994813215

Abstract:

Thermodynamic performance analysis is carried out on a flat plate solar thermal collector utilizing single and hybrid nanofluids. As heat transfer fluids, Fe_2O_4/water, Zn-Fe_2O_4/water hybrid nanofluids, and water are used, and its performance are compared based on the energy and exergy transfer rate. The thermo-physical properties are evaluated by regression polynomial model for all the working fluids. Developed codes in MATLAB solve the collector's thermal model iteratively, energy and exergetic performance are evaluated. The system was then subjected to parametric investigation and optimization for variations in fluid flow rate, temperatures, and concentrations of nanoparticles. The findings show that utilizing Zn-Fe_2O_4/water hybrid nanofluids with a particle concentration of 0.5 percent enhanced the solar collector's thermal performance by 6.6% while using Fe_2O_4/water nanofluids raised the collector's thermal performance by 7.83% when compared to water as the working fluid. While hybrid nanofluids give a better thermal alternative than water and single nanofluids, they have also produced a 5.36% increase in exergetic efficiency and an enhancement of 8.24 percent when used with Fe_2O_4/water nanofluids.

Keywords*: Solar collector, Hybrid Nanofluid, Zinc-ferrite/Water, Thermal performance, Exergy.*

1. Introduction

Solar energy is a free, widely available, and non-polluting fastest developing renewable energy source that may be utilized for power generation as well as heating applications like space heating, drying, and water heating. Domestic water heating consumes around 6% of total global energy consumption. Solar energy converting devices are capable of reliably converting the

absorbed solar radiation into heat energy for the working fluids. Flat plate collectors are economically feasible and extensively used solar thermal collectors. FPCs, on the other hand, have several design flaws, including low efficiencies, significant heat losses, and insufficient solar absorption efficiency. Enhancing the engineering and scientific restrictions of flat plate collectors may decrease the conventional energy generations and environmental issues associated with energy consumption.

"Nanofluid" has now become an eminent technique used enhancing the rate of energy transfer in the equipment for process heating applications. The experimental studies have been done to evaluate the thermo-physical properties of several nanofluids as a function of temperature (Esfe Mohammad Hemmat and Seyfolah Saedodin 2015; Abbasi et al.2016; Stalin et al.2017) because the engineering precision of energy converting devices is strongly reliant on the features of fluids used for heat transfer. Latest trends in manufacturing processes have enabled the production of nanoparticles. The magnetic, thermal, optical, mechanical, and electrical characteristics of nanoparticles ≤100 nm is superior. This gain is because of raise in surface area to volume ratio at grain boundaries, generated by a larger atom group (Chakraborty and Panigrahi 2020). The nanofluids created minimize the agglomeration and improve heat conductivity by dispersing nanoparticles in a base fluid (Hamilton and Crosser 1962).Surfactants added to nanofluids can dramatically decrease agglomeration. The study has been created the distributing micro-sized solid particles in working fluids to improve heat conductivity (Choi and Eastman 1995). Its use in practical applications has been restricted by the coagulation problem related to micro-sized elements.

The thermal conductivity enhances with the rise in temperature of the nanofluid, according to a large amount of research work on modeling, characterization, synthesis, convective and phase change heat transfer during the previous decade (Das et al.2003). Nanofluids outperform conventional fluids in terms of thermo-physical properties, heat transfer coefficient, thermal efficiency, and optical absorptivity, according to several studies (Bobbo et al.2012; Fedele et al.2012; Murshed et al.2005; Pak and Cho 1998; Said et al.2014; Sajid et al.2014; Vajjha et al.2009). Tyagi et al. [15] assessed the thermal performance of Al_2O_3/water-based nanofluids flowing through the tubes of direct absorption solar collector (DAC) known as a typical solar flat-plate collector, finding that the DAC is up to 10% more efficient. The author studied the influence

of CuO/water-based nanofluid on heat transfer characteristics of the FPSC in laminar flow conditions (Khin et al. 2016). Their research was based on calculating the thermal efficiency of nanoparticles as a role of their size and volume concentration size. It is revealed that as the concentration rises to 2.0%, the energy efficiency improves, but that the volume of the nanoparticles has little consequence on the performance. They found that at an optimum flow rate of 1.2 kg/min, two wt% CuO/water nanofluid improves FPSC efficiency by up to 5%. It has been reported that the 5% improvement in solar thermal collector performance with nanofluids as an absorbing medium (Otanicar et al.2010).

According to experimental and theoretical findings, nanofluids are very gifted and set to be substituted by usual fluids to improve solar collectors' efficiency. The improved thermal performance achieved by utilizing nano fluid has aided research in these sectors to find another way to reduce costs while increasing thermal performance. Hybrid nanofluids are a type of advanced fluid that has been produced to have a certain thermos physical characteristic. Because of the enhancement in thermal characteristics, the mixture of several nano powders with numerous base fluids, known as "hybrid nano fluid" (HNF), has been demonstrated apparently in many uses (Minea 2017). The author studied the numerous real-world applications that need dynamic compatibility between many factors, bringing hybrid nano fluid into the picture (Sarkar et al. 2015). This research aims to investigate whether a hybrid nano fluid could provide better thermal conductivity than separate nanofluids produced from Al_2O_3 and CuO powders using a hydrogen reduction method in a 90:10 ratio. According to measurements, the enhancement in thermal conductivity is comparatively lower with the rise in viscosity values (Suresh et al. 2011).

The study was focused the forced convective heat transfer for water, ethylene glycol, CNTs and Al_2O_3 based hybrid nanofluids by adopting the two-phase mixture model. The results reveal that utilizing ethylene glycol instead of water as a base fluid increases energy transmission (Labib et al.2013). This research work quantitatively investigated the Al_2O_3/water nanofluid at turbulent flow operating conditions with constant heat flux on the wall (Bianco et al.2011). They evaluated the findings in different concentrations using multi-phase models. This paper showed numerical simulations to analyze an Al_2O_3/water nanofluid using a novel method called the two-phase Eulerian model. It results that there is a greater agreement with experimental results when compared to a single-phase model (R. Lotfi et al. 2010). These studies investigated the laminar

convection of nanofluids using an Eulerian-Lagrangian approach (He et al. 2009; Bianco et al.2009). Their observations were compared to the available experimental data. The zinc/ferrite nanoparticles have improved value of stability which is advantageous for using longer periods. Temperature-sensitive ferro fluids are also used in the hybrid nanofluids under research, resulting in enhanced value of thermo-physical properties (Sundar et al.2017). Further, several reports have been published that adding ZnO and Fe_2O_4 particles on nanofluid shows a significant improvement in the value of thermal conductivity. According to the authors' knowledge, no research on Zn-Fe_2O_4/water hybrid nanofluids for evaluating solar collectors has been reported.

This research presents first and second law-based analysis of an FPSC using single and Zn-Fe_2O_4/water hybrid nanofluids. The user-developed code in MATLAB was used to analyze and enhance a proposed thermal model. The thermal model is developed based on the energy balance equations, updated to account for the effects of new single and hybrid nanofluids (Gupta et al.2020). Moreover, the thermal performance, exergy analysis, entropy generation, exergy destruction, and Bejan number of the nanofluids in the FPSC are evaluated with a functional evaluation of different operating temperatures, nanoparticle concentration, and flow rates. Finally, these parameters are subjected to impact analysis and optimization to get the collector's highest possible performance enhancement yield when used with each nanofluid.

2. Theoretical analysis

The FPSC is a solar collector consist an absorber plate and it was covered by transparent glass cover at top and thermal insulation at bottom for minimizing the heat losses. The riser tubes integrated with the absorber plate to collect and transfer the heat to the working fluid. The solar radiation penetrates over the transparent cover made up of glass and strike over the surface of the absorber plate, which has an extremely higher rate of absorptivity. The absorber plate is designed to collect the maximum amount of solar energy possible. By minimizing the stationary air formulation between the glass cover and the heated absorber plate, decreases absorber plate heat loss caused by the wind. It also aids in decreasing the collector's radiative heat losses by making wave length of in the range of 3-100 μ released by the heated plate. The nano fluid running within the risers absorbs a large amount of heat energy received by the hot absorber plate. Figure 1 represents astructure of the FPSC. The size and characteristics of the FPSC are listed in Table 2.

This section includes the equations that were utilized to describe the flat plate collector (FPC). The system, nanofluids and fluid flow area are all detailed and modelled in the following sections. The analytical work is carried out with an assumption that the system properties are not varies with time and the heat flows are homogeneous. In theoretical analysis, all of the risers have equal flow rate, whereas the central axis connecting the risers and absorber plate are both in the same path (refer Fig. 1)

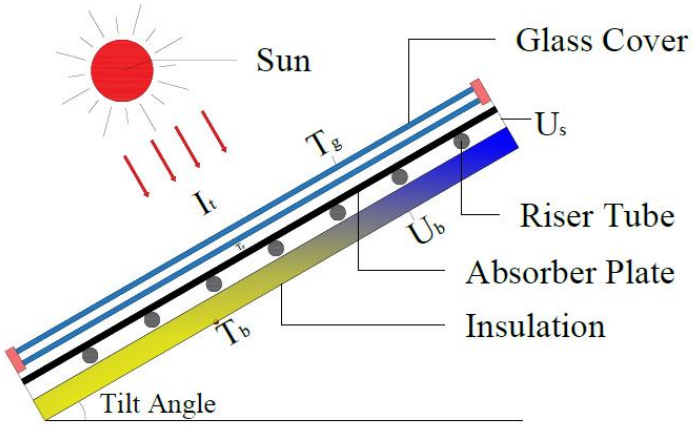

Fig.1. Schematic layout of flat plate solar collector

Table 1

Design parameters for the solar collector under investigations

Sl.No	Parts	Specifications
1	Collector area (A_c)	2 m^2
2	Riser tubes length (L)	2000 mm
3	Collector tilt angle (β)	15°
4	Back insulation thickness (t_b)	50 mm
5	Side insulation thickness (t_s)	25 mm
6	Absorber plate thickness (t_p)	0.454mm
7	Absorber plate thermal conductivity (k_p)	384 W/m K

8	Absorbance(α)	0.962
9	Transmittance(τ)	0.87
10	Number of glass cover (N)	1
11	glass covers emissivity of (ε_c)	0.88
12	Ambient temperature	25°C
13	Emissivity of absorber plate (ε_p)	0.92
14	Distance between risers (9 Nos) (W)	95mm
15	Riser pipeinner diameter (D_i)	9.5mm
16	Riser pipeouter diameter (D_o)	10mm
17	Diameterof the header pipe(D)	25mm
18	Speed of the wind (V_w)	1 m/s
19	Incident solar radiation (I_t)	800 Wm^{-2}

130

131 **2.1 Energy Analysis.**

132 The useful gain that transfer to the working fluid of flat plate collector is evaluated by using
133 the Eq. (1) (Ozil and Yaşar 1987):

134 $$Q_u = I_t.A_c.(\tau\alpha) - U_L \quad (1)$$

135 In the equation 1 I_t represents solar energy input to the FPSC per area, A_c indicates area of absorber
136 plate that receives the input energy, $(\tau\alpha)$is the combined influence of transmittance of glass cover
137 and the absorptance of absorber plate surface and $U_L$shows the overall loss coefficient of the
138 collector.

139 A flat plate collector's efficiency (η) is defined as the proportion of usable energy (Q_u) to
140 total incident solar energy on the solar collector area:

141 $$\text{Efficiency} = \frac{Q_u}{A_c I_t} \times 100 \quad (2)$$

The energy loss from the collector is shown in Q_l. Eq. (3) (Duffie and Beckman 2013), it includes all the losses happens by the three modes of heat transfer.

$$Q_l = U_l . A_C \left(T_p - T_o\right) \tag{3}$$

T_p andT_o indicate absorber plate and the surrounding environment temperature, respectively. Further, Ut, Us and U_b represents top loss, bottom loss and side loss from the systemThe summation of all three losses yields the total heat loss from the system.

$$U_l = U_t + U_{bc} + U_s \tag{4}$$

Eq.(5) gives the top loss coefficient (Ut);

$$U_t = \frac{1}{\frac{N}{\frac{C}{T_p}\left[\frac{T_p - T_o}{N - f}\right]0.31 + \frac{1}{h_c,\infty}}} + \frac{\sigma\left(T_p{}^2 - T_o{}^2\right)\left(T_p - T_o\right)}{\frac{1}{\varepsilon_{pl} + 0.0425N\left(1-\varepsilon_{pl}\right)} + \frac{2N + f - 1}{\varepsilon_g} - N} \tag{5}$$

where

ε_{pl} = Absorber plate Emissivity

ε_g = Glass cover emissivity

σ = Stefan–Boltzmann constant

h_c = Wind heat transfer coefficient

N = quantity of glass cover

The convective heat loss coefficient between FPSC and ambient air are evaluated by the Eqs. (6)-(8) (Ozil and Yaşar 1987). Further, the constants f and C is given by

$$h_c = \frac{8.6 V_W{}^{0.6}}{L^{0.4}} \tag{6}$$

$$f = \left(1 + 0.056N\right)\left(1 - 0.04h_c + 0.0005h_c{}^2\right) \tag{7}$$

$$C = \left(1 - 0.00883\beta + 0.0001298\beta^2\right)365.9 \tag{8}$$

Where,V_w and L are the wind speed and collector length, respectively. The heat loss happens at the bottom of the collector is directly proportional to the thermal conductivity (k_b) of the insulation, bottom heat loss coefficient (h_b) and indirectly proportional to the thickness of insulation (t_b). It is evaluated using the relation as follows (Mahian et al.2014):

$$U_{bc} = \frac{1}{\frac{t_b}{k_b} + \frac{1}{h_b}} \tag{9}$$

The energy loss from the edges of FPSC is given by Eq. (10).

$$U_s = \frac{1}{\frac{t_s}{k_s} + \frac{1}{h_s}} \frac{A_s}{A_c} \tag{10}$$

Where, t_b denotes the thickness of the insulation in the bottom region, t_s denotes the thickness of the insulation edge, and k_b denotes the thermal conductivity of the insulation in the bottom surface. k_s is the insulation's thermal conductivity at the margins and A_s is the area of the edges' surface.

U_t and U_l are depending on the temperature of the absorber plate T_p, as shown in Eq.(11). As a result, Eq.(11) (Kalogirou 2009) is provided as an equation to determine the plate temperature:

$$T_p = T_{in} + \frac{Q_u}{A_c F_R U_L}\left(1 - F_R\right) \tag{11}$$

Where F_R stands for heat removal coefficient and may be computed using the following Eq.(12) (Kalogirou 2009)

$$F_R = \frac{\dot{m} C_p}{A_c U_L}\left[1 - \exp\left(-\frac{U_L F \dot{A}_c}{\dot{m} C_p}\right)\right] \tag{12}$$

In the Eq.(13) (Kalogirou 2009), F' represents the collector efficiency factor. The following formula can be used to compute the factor:

$$F' = \frac{\frac{1}{U_L}}{W\left[\frac{1}{U_L (W - D) F} + \frac{1}{\pi D_i h_f}\right]} \tag{13}$$

In the above equation W indicates the tube spacing, D represents riser tube diameter at outer side, h_f indicates coefficient of heat transfer and D_i denote, riser tube diameter at inner side respectively. The fin efficiency of the collector is evaluated using the relation as follows (Kalogirou 2009):

$$F = \frac{\tanh\left[(W-D)m/2\right]}{(W-D)m/2} \tag{14}$$

Where, $m=\sqrt{\frac{U_L}{k_p t_p}}$ in which thermal conductivity and absorber plate thickness are represented by kp and tp, correspondingly.

For laminar flow conditions, the internal heat transfer coefficient (h_f) is calculated using Eq.(15).

$$h_{fi} = \frac{48 k_{nf}}{11 D_i} \tag{15}$$

The Eq.(16) and Eq.(17) give the Reynolds and Prandtl numbers, expressed in the following way.

$$\mathrm{Re} = \frac{4\dot{m}_r}{\pi D_i \mu_{nf}} \tag{16}$$

$$\mathrm{Pr} = \frac{\mu_{nf} C_{p,nf}}{k_{nf}} \tag{17}$$

Where, ($\dot{m}_r$) seem to be the flow rate (kg/s) of nano fluid riser tube. The Eq.(18) can be used to determine the temperature of working fluids at their outlet.

$$T_{out} = T_{in} + \frac{Q_u}{\dot{m} C_p} \tag{18}$$

2.2 Exergy Analysis

Exergy refers to the transformation of available energy into productive work or energy and so specifies the compactness of the thermal system. Exergy efficiency is the maximum amount of useful work that a system may generate, and it is defined as follows:

$$\eta_{ex} = \frac{E_u}{E_{sun}} \tag{19}$$

Where, E_u and E_{sun} are the collector's and sun's exergy outputs, respectively. Eq.(20) (Okonkwo et al.2019; Ratlamwala et.al.2019) can be used to determine solar exergy:

$$\dot{E}_{sun} = A_c I_t \left(1 - \frac{4}{3}\left(\frac{T_o}{T_{sun}}\right) + \frac{1}{3}\left(\frac{T_o}{T_{sun}}\right)^4\right) \tag{20}$$

Eq. (21) compensates for the irreversibility caused by pressure losses and heat transfer in the system (Ratlamwala et.al.2019) , which may be used to calculate the collectors' exergetic output:

$$\dot{E}_u = \dot{Q} - \dot{m} C_p T_o . \ln\left(\frac{T_{out}}{T_{in}}\right) - \dot{m} T_o \frac{\Delta P}{\rho_f T_f} \tag{21}$$

Where, P is the pressure decrease in the system

2.3 Entropy generation for FPSC

The work lost (W_{lost}) to the environment is required to calculate the collector's entropy generation rate and its relationship is represented by Eq.(22) (Okonkwo et al.2019).

$$\dot{S}_{gen} = \frac{\dot{w}_{lost}}{T_o} = \frac{\dot{E}_d + \dot{E}_{loss}}{T_o} \tag{22}$$

The exergy loss to the environment is calculated as follows (Mahian et al.2014).

$$\dot{E}_{loss} = U_l A_c \left(T_P - T_o\right)\left(1 - \frac{T_o}{T_P}\right) \tag{23}$$

It gives the quantity of energy lost (Ed) in the collector like a function of device irreversibility (Padilla et al.2014).

$$\dot{E}_d = \dot{E}_{d,\Delta T_s} + \dot{E}_{d,\Delta P} + \dot{E}_{d,\Delta T_f} \tag{24}$$

The exergy lost due to friction that happens between flowing fluid and collector wall surfaces, enhances the drop in pressure and pumping power. It is calculated as follows:

$$\dot{E}_{d,\Delta P} = T_o \dot{m} \frac{\Delta P}{\rho} \frac{\ln\left(\frac{T_{out}}{T_a}\right)}{\left(T_{out} - T_{in}\right)} \tag{25}$$

The loss of exergy occurs due to temperature difference between the Sun (T_s) and the heated absorber plate (T_p) is $\dot{E}_{d,\Delta T_S}$ which is given by (Padilla et al.2014).

$$\dot{E}_{d,\Delta T_s} = (\tau\alpha)_{eff} I_t A_c T_O \left(\frac{1}{T_p} - \frac{1}{T_{sun}}\right) \tag{26}$$

The exergy lost due to movement of the hot fluid inside the collecting tubes $\dot{E}_{d,\Delta T_{fl}}$ can be evaluated using the following formula:

$$\dot{E}_{d,\Delta T_f} = \dot{m} C_p T_o \left(\ln\left(\frac{T_{out}}{T_o}\right) - \frac{\left(T_{out} - T_{in}\right)}{T_P}\right) \tag{27}$$

The entropy generation is evaluated by using the Eqs.(21)–(25) and Eq.(28).

$$\dot{S}_{gen} = \underbrace{E_{loss} + (\tau\alpha)_{eff} I_t A_c T_O \left(\frac{1}{T_p} - \frac{1}{T_{sun}}\right) + \dot{m} C_p T_o \left(\ln\left(\frac{T_{out}}{T_o}\right) - \frac{\left(T_{out} - T_{in}\right)}{T_P}\right)}_{\left(\dot{S}_{gen}\right)_H} + T_o \dot{m} \frac{\Delta P}{\rho} \frac{\ln\left(\frac{T_{out}}{T_a}\right)}{\left(T_{out} - T_{in}\right)} \tag{28}$$

The Bejan number indicates the fraction of entropy generation that happens in the system only due to the heat transfer process. it is evaluated by

$$Be = \frac{\left(\dot{S}_{gen}\right)_H}{\dot{S}_{gen}} \tag{29}$$

3. Determination of Hybrid Nanofluids Properties

The correlations used to predict and characterize the thermal characteristics of Zn-Fe_2O_4 Hybrid Nanofluids were obtained from the literature. The base fluid (bf) was used to define nanofluid, which consisted of a hybrid nanoparticle of Zn (n_{p1}), Fe_2O_4 nanoparticle (n_{p2}), and the hybrid nanofluids (h_{nf}). The effect of using conventional single nanofluid at medium and high inlet temperatures was investigated for any nanoparticle with a particle volume fraction (φ) of 0.5

percent, while the calculated results for hybrid nanofluids occurred under different conditions for two distinct methods with a volume concentration (φ_{tot}) of 0.5 percent. This overall particle volume fraction was split into 50:50 mixing fractions, resulting in a volume fraction of 0.25% for each nanoparticle. The total volume fraction is defined by the following equation, which may be used to characterize nanofluid in single or hybrid nanofluids.

The total volume fraction of hybrid nanofluids with conventional fluids obtained, as illustrated in Eq. (30) (Takabi et al.2014).

$$\varphi_{total} = \varphi_{np1} + \varphi_{np2} \tag{30}$$

The density of hybrid nanofluids is described in Eq. (31) and it has been discussed in several research papers (Bellos and Tzivanidis 2018; Rasih et al. 2019).

$$\rho_{hnf} = \varphi_{np1}.\rho_{np1} + \varphi_{np2}.\rho_{np2} + (1-\varphi_{total}).\rho_{bf} \tag{31}$$

To address single and hybrid Nanofluids, the specific heat capacity formula in Eq. (32) is utilized. Therefore, its capacity to cover a wide variety of particle volume concentrations as well as its application in various nanofluid types, this formula has been frequently utilized in the literature (Rasih et al. 2019).

$$C_{p,nf} = \frac{\varphi_{np1}.\rho_{np1}.C_{p,np1} + \varphi_{np2}.\rho_{np2}C_{p,np2} + (1-\phi_{total}).\rho_{bf}.C_{p,bf}}{\rho_{hnf}} \tag{32}$$

The thermal properties of nanofluids had been calculated using Maxwell correlation, as indicated in Eq. (33) (Rasih et al. 2019; Maxwell 1873), which was expanded to include hybrid and single nanofluids.

$$k_{hnf} = \frac{\frac{\varphi_{np1}.k_{np1} + \varphi_{np2}.k_{np2}}{\varphi_{total}} + 2.k_{bf} + 2.(\varphi_{np1}.k_{np1} + \varphi_{np2}.k_{np2}) - 2.\varphi_{total}.k_{bf}}{\frac{\varphi_{np1}.k_{np1} + \varphi_{np2}.k_{np2}}{\varphi_{total}} + 2.k_{bf} - 2.(\varphi_{np1}.k_{np1} + \varphi_{np2}.k_{np2}) + \varphi_{total}.k_{bf}} \tag{33}$$

The dynamic viscosity of the nanofluid was estimated using the Brinkman model correlation, as stated in Eq. (34) (Brinkman 1952),

$$\mu_{hnf} = \mu_{bf}\left(\frac{1}{(1-\varphi^{2.5})}\right) \tag{34}$$

The correlations that were utilized to describe the thermal characteristics of hybrid nanofluids were often taken from the earlier work, by (Mwesigye and Huan 2015) investigation pointed out. The

following equations are applied for evaluating the properties of heating fluid is described below (Mwesigye and Huan 2015).

$$C_{pbf} = 1.10787 + 1.70736.10^{-3}T \quad (35)$$

$$\rho_{bf} = 0.1291\times10^{-3} - 1.52115\,T + 0.179133.10^{-2}T^2 - 1.671545\,T^3 \quad (36)$$

$$k_{bf} = 0.9013 - 1.88053\times10^{-4}T \quad (37)$$

Eq. (38) for 343 ≥T ≥ 233.15 K and Eq. (39) for 673.15 ≥T ≥343 K illustrate characteristics of dynamic viscosity as function of inlet temperature of the fluid.

$$\mu_{bf} = 5.14\times10^{4} - (9.6165.10^{2}T) + (7.502\times T^{2}) - (0.31246.10^{-3}\times T^{3}) + (0.7322.10^{-6}\times T^{4}) - (0.01463.10^{-9}\times T^{5}) + (0.47562.10^{-10}\times T^{6}) \quad (38)$$

$$\mu_{bf} = 9.8856.10 - (7.309\times10^{-1}\times T) + (0.221917\times10^{-2}\times T^{2}) - (0.342377\times10^{-5}\times T^{3}) + (0.26683\times10^{-8}\times T^{4}) \quad (39)$$

With respect to the findings, prior fundamental correlations described in this part is used to describe the thermal characteristics of these revised heat transfer fluids in terms of their capacity to forecast an acceptable outcome, as well as the lack of unique relationships to include oil in a high temperature range. In this work, the Nusselt number was utilized to address the hybrid nanofluids, whether it was for the conventional fluids, a single nanofluids, or to estimate the fluid's heat transfer coefficient. Because of its capability to cover diverse kinds of nanofluids, including alkali metals, Gupta's relation, as indicated by Eq.(40), was used to evaluate the Nusselt number for the hybrid nanofluids. The correlation was valid up to the volume concentration ratio of 0.1-0.5.%. This equation is applied to the Nusselt number for the hybrid energy system as a consequence of this investigation (Gupta et al.2015).

$$Nu = 0.2437\,\mathrm{Re}^{0.4896}\,\mathrm{Pr}^{0.2847}\,\varphi^{0.1017} \quad (40)$$

To include the resulting value of distinct monotypes, the Nusselt number for single nanofluid was calculated using Maiga's correlation. As a result, the validity of this equation has been demonstrated for a variety of nanoparticle kinds in a laminar environment. Equation 41 is utilized to calculate the Nusselt number is describing below (Maiga et al.2005).

$$Nu = 0.086\,\mathrm{Re}^{0.55}\,\mathrm{Pr}^{0.5} \quad (41)$$

Table 2. Properties of the base fluid, Zn and **Fe_2O_4** nanoparticles

Sl.No	Properties	Water	ZnO	Fe_2O_4
1	Thermal conductivity (W/mK)	0.52	29	80.4
2	Specific heat (J/kg K)	4.187	514	670
3	Density (kg/m3)	1000	5600	5180

4. Results and discussion

The performance assessment of Zn-Fe_2O_4/water nanofluids was theoretically studied and the results obtained in this research work are presented in this section. Moreover, the second law analysis of the Zn-Fe_2O_4/water with various concentrations with respect to different mass flow rates has been discussed.

Fig. 2 elucidates the variation of collector thermal efficiency with respect to the mass flow rate for different concentrations of hybrid nanofluids. The studies were accompanied by a constant solar thermal intensity and an atmospheric temperature of 1000 W/m^2 and 25°C. The inlet collector temperature was assumed to be 27°C. The most influencing parameter which effects the solar thermal collector performance are mass flow rate, charactertics and concentration of nano particles. For all types of working fluids, the collector's thermal efficiency improves as the mass flow rate increases. The mass flow rate is exactly proportional to the Reynolds number as a result of this. This is significant because the heat capacity of the flowing fluid increases with Reynolds number and lower the mean wall temperature of the solar collector, lowering system thermal losses.

It can be observed that the system efficiency of FPSC with Fe_2O_4/water nanofluid have significant performance improvement as it compared with water flows at a mass flow rate of 0.01 to 0.1kg/s. However, the system with a hybrid nanofluid composed of zinc and ferrite appears to be superior to the ferrite nanofluid, indicating that the zinc addition with ferrite nano-particles synergistically enhances the system's performance. The collector efficiency has increased significantly with the increase of Zn-Fe_2O_4/water hybrid nanoparticles in water. It is obvious that the efficiency surged steeply up to a value of 0.03 kg/s and then slowly till 0.1 kg/s. The increment in performance was insignificant beyond value of 0.06 kg/s. Furthermore, the highest collector

efficiency for the FPSC system with a 0.5 percent concentration of Zn-Fe_2O_4/water hybrid nanofluids was increased by 6.6% when compared to Fe_2O_4/water nanofluids. Because nanofluids have a greater thermal conductivity, reduces the overall thermal resistance throughout the FPSC, the reduces the local thermal barriers will decreases considerably at higher flow conditions.

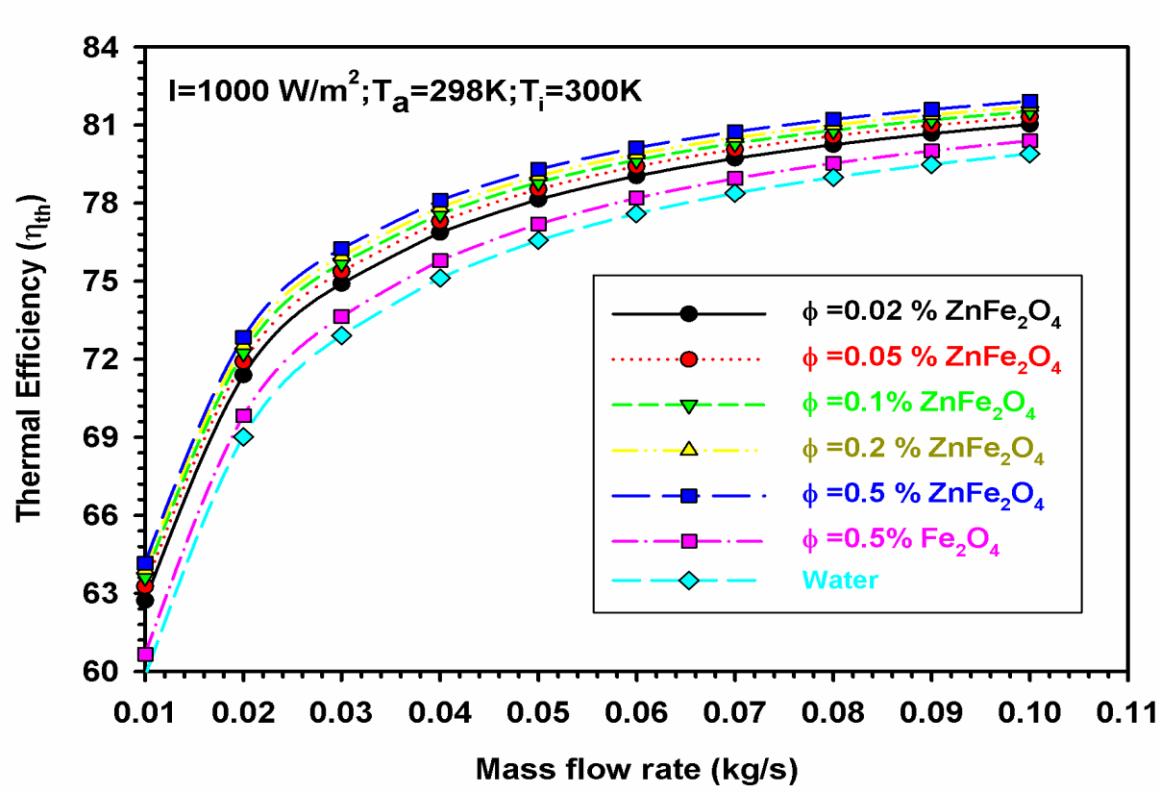

Fig. 2. Collector efficiency v/s mass rate.

The improvement in heat transfer coefficient of the system with the increment in rate of flow rate is depicted in Fig.3. The heat transfer coefficient was weak for the water based FPSC system. The FPSC system with Fe_2O_4/water nanofluid shows that the better heat transfer coefficient was raised by 25.8% compared to conventional fluid. But, the system with hybrid nanofluid is significantly high related to the conventional fluid and Fe_2O_4/water nanofluid systems for the corresponding mass flow rates. Improved heat transfer properties were evaluated by the viscosity of nanofluids and effective thermal conductivity. The heat transfer coefficient enhances with the raise in the concentration of hybrid nanofluids. The higher heat transfer coefficient can be characterized for the FPSC system with a 0.5% hybrid concentration at a flow rate of 0.1 kg/s. When compared to Fe_2O_4/water nanofluid for the identical operating conditions, the convective

heat transfer coefficient of Zn-Fe_2O_4/water hybrid nanofluid was increased by 10.3% to 42.05% for the ϕ values varying from 0.02 to 0.5 percent. This improvement is shown to be enhanced at higher temperatures, implying that more effective energy is generated at these temperatures due to a lower heat loss coefficient, resulting in increased efficiency. As a result, it's easy to see how the greater concentration and fluid flow rate would improve the system's heat transfer coefficient.

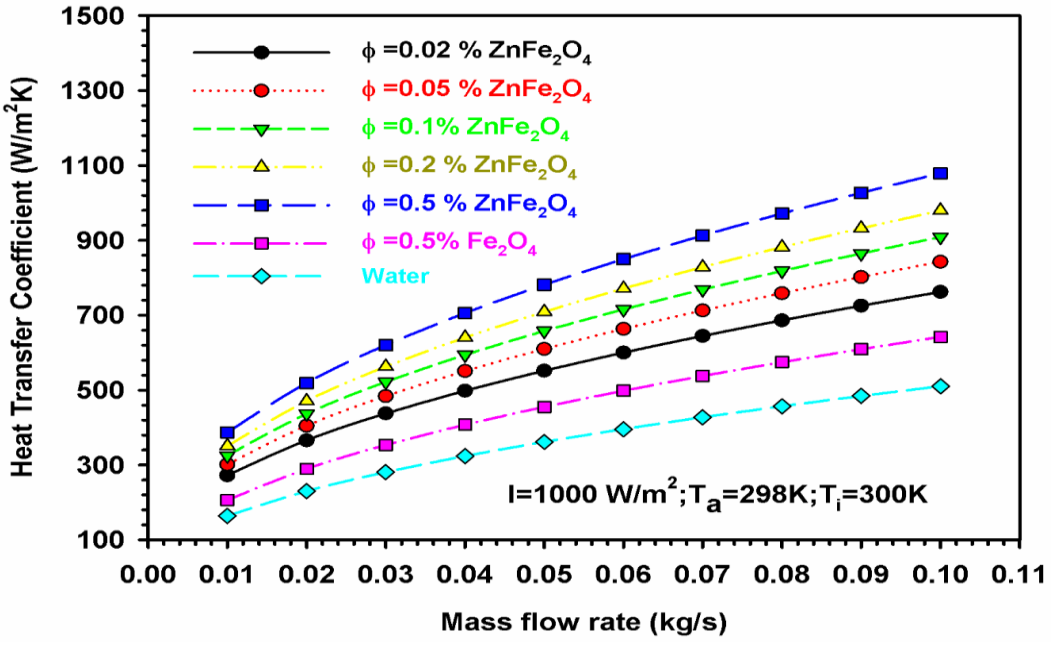

Fig. 3. Deviation heat transfer coefficient as a result of mass flow rate and volume concentration

The variations in first law and exergy efficiency pertaining to the Reduced Temperature Parameter (RTP) are plotted in Fig.4. The system with three types of fluids, namely, water, 0.5% Fe2O4/water nanofluid, and 0.5% Zn-Fe_2O_4/water hybrid nanofluid, is taken for consideration for a constant solar heat flux of 1000 W/m^2 and a mass flow rate of 0.01 kg/s. The performance of the collector decreases with an increase in the reduced temperature parameter. This occurs because as RTPs increase, the temperature of the absorber plate rises, increasing heat losses to the atmosphere. Further, when the operating temperature of the FPSC increases, the density and viscosity of fluids seem to be reduced, which reduces the performance of the collector. Hybrid nanofluid with a 0.5% concentration is considered for this plot owing to its contribution to an 8.4%improvement in collector efficiency as compared with water due to the enhancement in convective heat transfer coefficient. Energy efficiency, on the other hand, showed a steadily rising trend in relation to the

increase in the reduced temperature parameter. This rise occurred due to that presence of more thermal energy to be converted into useful heat gain in the collector. While the black absorber plate attains thermal equilibrium with the sun, the exergetic performance of the system increases and reduces the energy destruction rate. The comparison study between the three working fluids results that, the hybrid nanofluid has the highest exergetic performance due to its superior thermal conductivity qualities. The maximum exergetic performance of 5.36 % was obtained for the reduced temperature parameter of 0.03 Km^2/W. Further, a rise in mass flow rate decreases the performance due to a rise in pumping power.

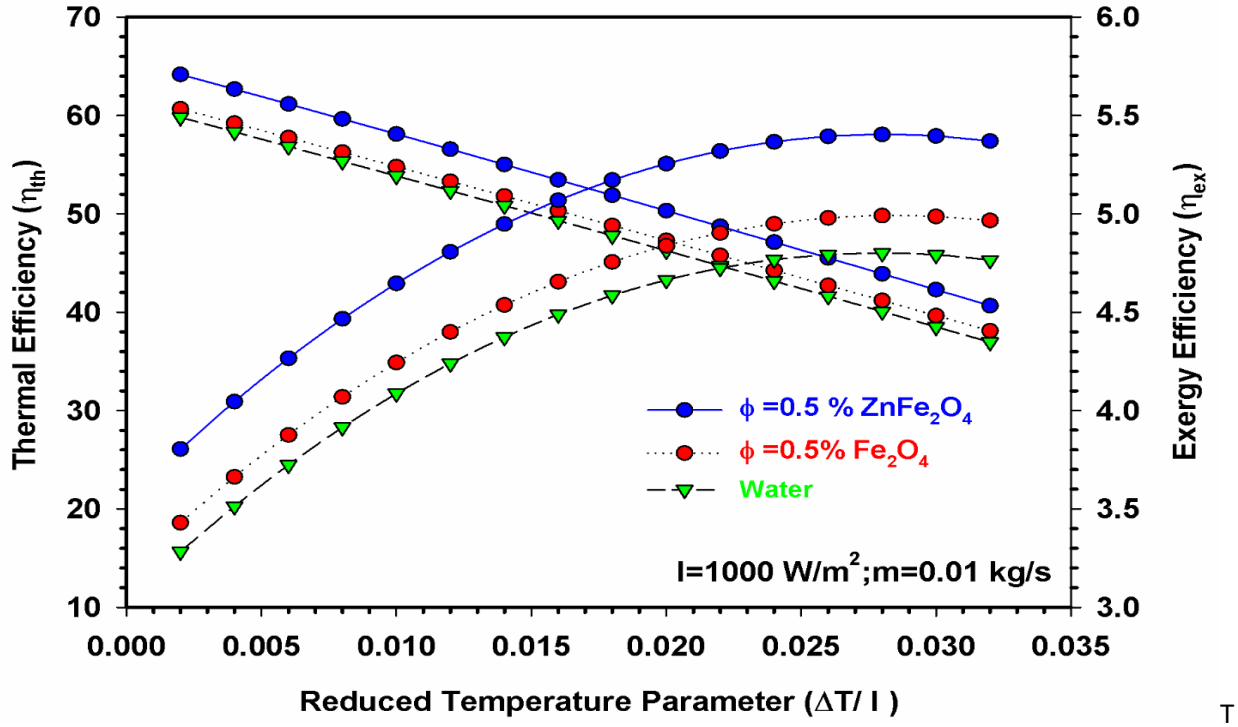

T

Fig. 4. Exergy and thermal performance of FPSCas a function of RTP

Figure 5 portrays the variation in exergy efficiency with regard to mass flow rate and volume concentration of Zn-Fe2O4/water hybrid nanofluids. A value of 3.73 % exergy efficiency was recorded for a mass flow rate of 0.025 kg/s and a volume concentration () of 0.5. The maximum exergy performance was obtained with the minimum value of flow rate and maximum volume concentration. The exergy efficiency shows a declining trend with the mass flow rate and improving fashion with the volume concentration of hybrid nanofluids. This occurs because the exergy destruction rate improves with increase in fluid flow rate owing to the limited temperature

differential between the FPSC components such as the sun, absorber plate, absorber tube, and working fluid. Increased pressure drop at greater flow rates, on the other hand, lowers average fluid temperature and increases exergy destruction owing to friction.

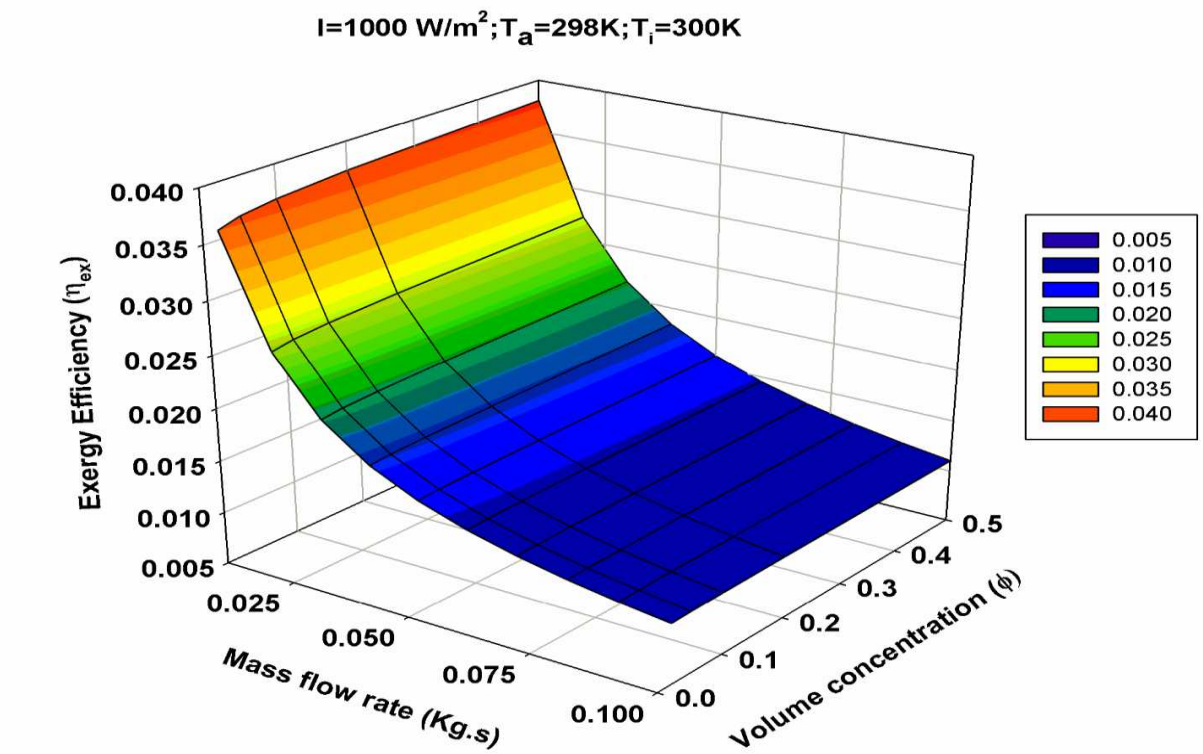

Fig. 5. Influence of fluid flow rates and particle volume concentrations on exergy efficiency

Figure 6 depicts the exergy losses and exergy destruction of FPSC system with respect to fluid flow rate for the collector operates with various working fluids. The investigation was carried out at a steady solar heat flux of 1×10^3 W/m^2 with the atmospheric temperature of 25°C and the inlet collector temperature was assumed to be 27°C. It is vividly understood that the destruction of exergy monotonically raised with the increment in fluid flow rate inside the riser tubes. The increment was initially significant and became less at the higher fluid flow rates. It indicates that the generation of entropy was high at the augmented mass flow rates. On the other hand, the exergy loss of the FPSC system drops with increased mass flow rates. Similar to the exergy destruction, the loss in exergy was considerably reduced till the value of 0.04 kg/s and less significant afterwards. When the mass flow rates are raised, the heat transfer to the ambient are reduced because the Reynolds number is increased, leads to rapidly removes energy from the walls of the solar collector's absorber. Compared to the nanofluids, the exergy destruction and exergy loss were

expressively higher for the water. Further, Zn-Fe_2O_4/water hybrid nanofluid recorded lesser exergy destruction and exergy loss with the increment in mass flow rate compared to the nanofluid containing Fe_2O_4 nanoparticles. The fluid decreases exergy destruction and losses by a maximum of 3.7% when compared with water. On the whole, the hybrid nanofluid was assisted to reduce the irreversibility of the FPC system substantially, compared to other fluid fluids. As the Reynolds number raises considerably, the heat resistance within the collector decreases.

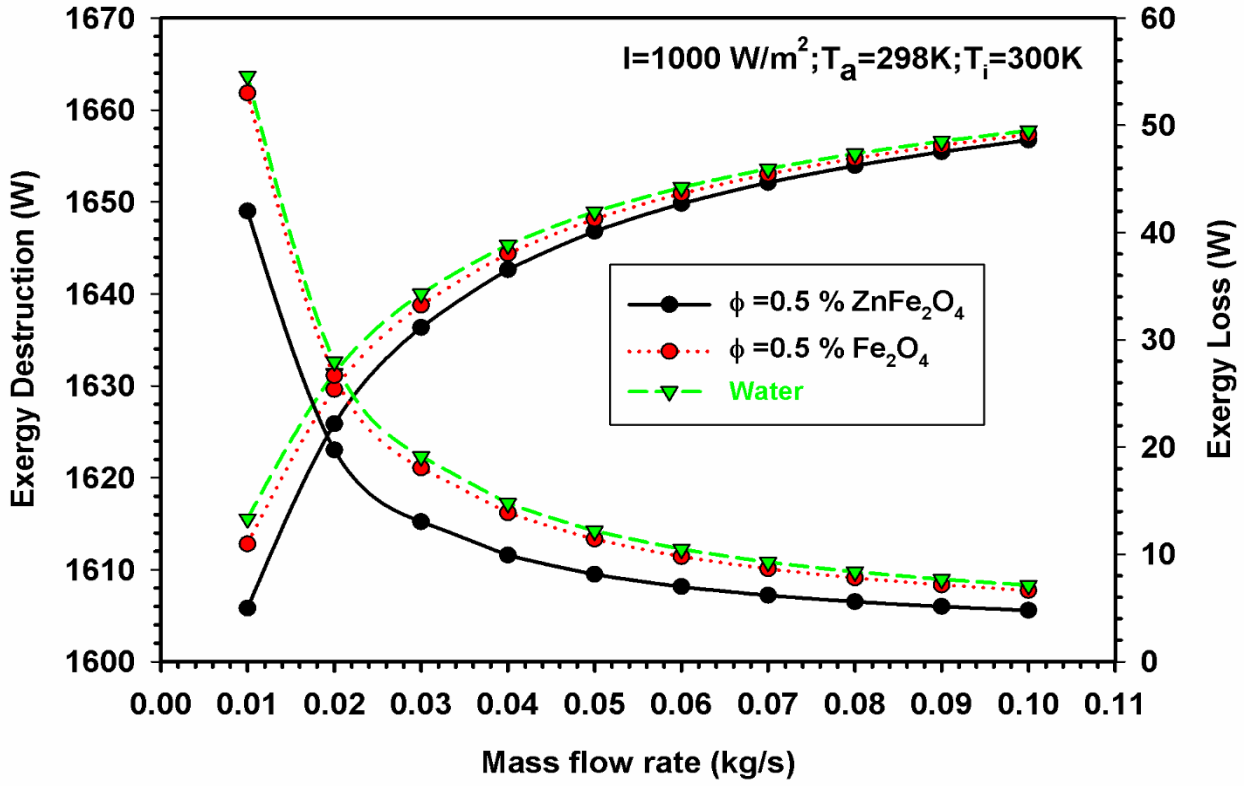

Fig. 6. Influence of mass flow rate on Exergydestructionandexergy losses

At a constant solar thermal intensity of 1×10^3 W/m^2 and a fluid flow rate of 0.01 kg/s, Fig.7. illustrates destruction in exergy values and losses in exergy values as a function of ΔT/I. Among the exergy input values only around 3–5.5% is converted to usable energy, since the rest is lost due to exergy losses and exergy destruction factors. As the sun's energy is collected by the collector, the system's total exergy is depleted. It's because of the large thermal gradient among the solar collector and the source; as the temperature variation decreases, the destruction inexergy is minimized to a lesser extent. It's also been found that utilizing hybrid Zn-Fe_2O_4/water nanofluids

reduces the force of losses in exergy of the FPSC by maximum of 2.84 percent. Fe_2O_4/water nanofluids have also been shown to effectively reduce the rate of irreversibilities with in process. The increased thermal conductivity properties of nanofluids are the reason for this. However, when it comes to exergy losses in the system, Zn-Fe_2O_4/water hybrid nanofluids are a superior alternative.

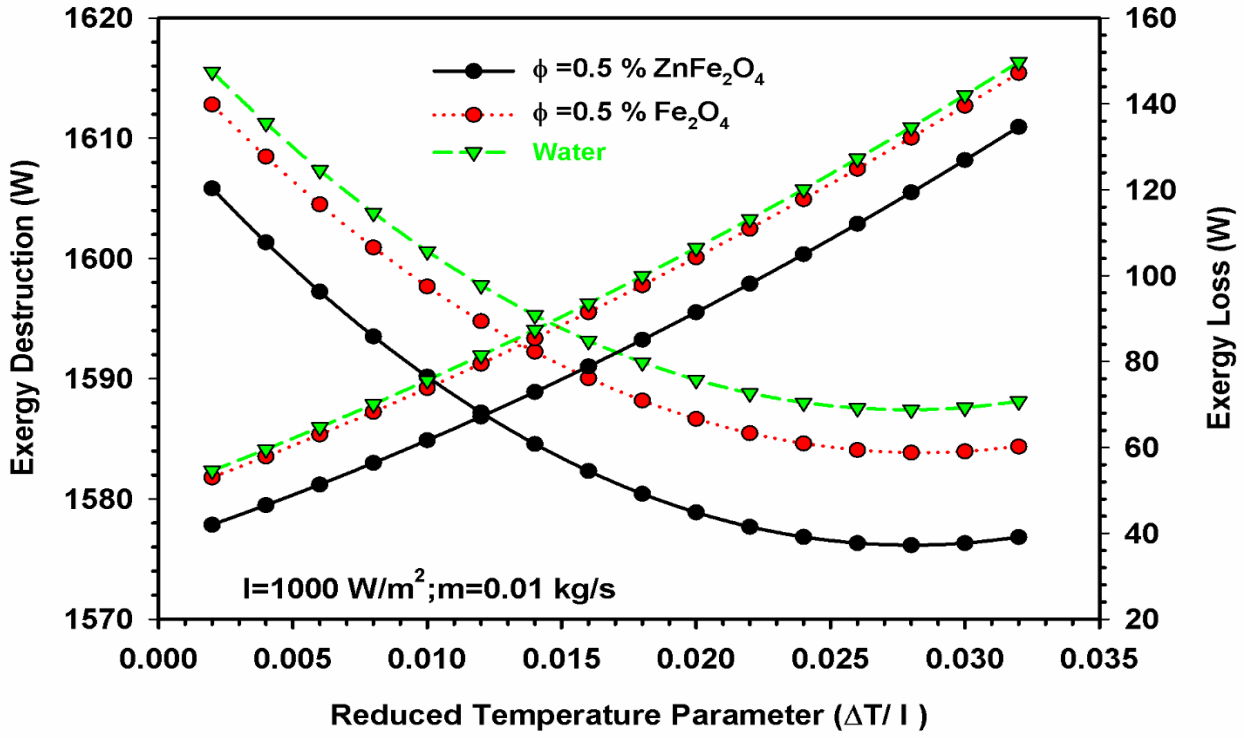

Fig. 7. Exergy losses and destruction as a function of (ΔT/I)

Figure 8 depicts the changes in entropy generation and Bejan Number for the Reduced Temperature parameter. It is also fascinating to note that the accumulation of entropy gradually decreases in water for 0.5% Fe_2O_4 nanofluid as well as for 0.5% Zn-Fe_2O_4/water hybrid nanofluid as the working fluids have increased the reduction temperature parameter $(T_i - T_a)/I_t$ .The inability of a system to convert available energy into useful tasks is shown by entropy generation. It is not typically advised to generate entropy at a faster rate. The entropy generation rate for the 0.5 percent Zn-Fe_2O_4/water hybrid nanofluid is 5.39 W/K, whereas it is 5.41 W/K for 0.5 percent Fe_2O_4/water nanofluids and 5.43W/K for water, respectively, among the selected working fluids. The physical significance of the Bejan number is shown in Eq (29). It is a non-dimensional number that represents the proportion of entropy generated by thermal energy transfer to the overall entropy

generated by thermal energy transfer plus irreversibility induced internally by pressure drop and frictional losses happens at adiabatic conditions. A shift toward a greater Bejan number indicates that the system's dynamic responsiveness has improved. The Bejan number falls when the reduction temperature parameter is increased for a constant particle volume concentration. Because entropy generation due to ΔP is less than that provided by irreversibility, the decrease in Bejan number is progressive rather than rapid.

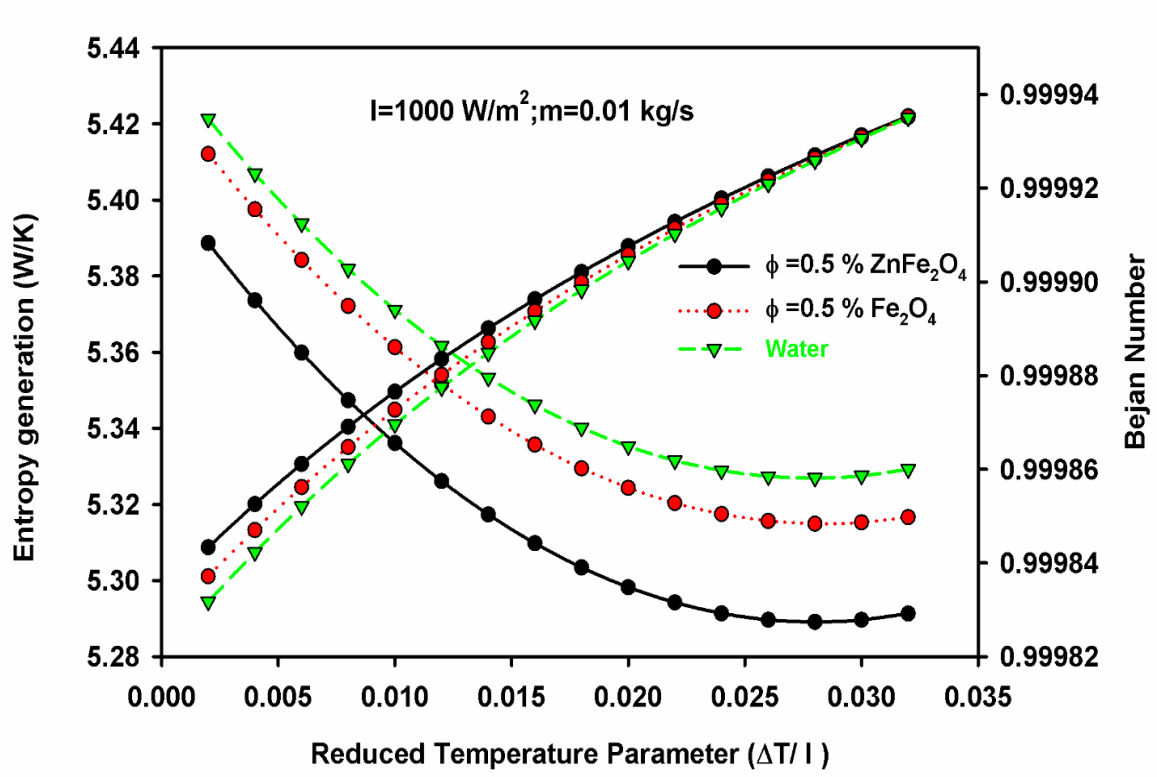

Fig. 8. Influence of ΔT/I on Bejan number and entropy generation of FPSC

Conclusions

An analytical study was performed to assess the effectiveness of a thermal flat plate solar collector using water, Fe_2O_4/water nanofluid, and Zn-Fe_2O_4/water hybrid nanofluid as working fluids at various flow rates for varied volume concentrations. The developed regression polynomial form was use to calculate the thermal properties of all the working fluids. On the use of MATLAB codes, thermal model for the FPSC was solved and the first and second law-based performances were evaluated.

The following points highlight the key conclusions in the results.

- At a nanoparticle concentration of 0.5%, Zn-Fe2O4/water hybrid nanofluid provides a thermal enhancement of 6.6 % in the collector when compared to Fe_2O_4/water nanofluid. When compared to water, single nanofluids improve the collector's thermal performance by 7.83 %.
- While hybrid nanofluids give a superior thermal alternative than water and single nanofluids, they also showed a8.24% increase in exergetic efficiency over Fe_2O_4/water nanofluids.
- Whereas nanoparticles improve the performance of heat transfer fluids, there is an best possible volume concentration of nanoparticles beyond which its usage in a fluid is becomes less helpful to the energy and exergy transfer rate.
- The convective heat transfer flux in the flow area is significantly increased by nanofluids. Fe_2O_4/water nanofluids and Zn-Fe_2O_4/water hybrid nanofluids both show a 25.8% and 52.6% increase in heat transfer coefficient, respectively.
- Exergy destruction due to energy transfer between the FPSC and the source attributed for 13.8% of total exergy destruction across the FPSC, whereas destruction in exergy due to friction recorded for the lower amount of exergy destruction at 0.05 % of total exergy destruction.
- The greater enhancement in nanofluid thermal conductivity values, significantly reduces the of entropy generationrate in the system as the nanoparticles concentration in the fluid increases.
- The magnitude of entropy formulation in the FPSC increases when the mass flow rate is raised due to higher pumping losses happens in the system.
- The magnitude of mass flow rate are higher, the Bejan number is reduced due to the raise in pumping power losses.

REFERENCES

Abbasi S, Zebarjad SM, Baghban SHN, Youssefi A, EkramiKakhki MS (2016) Experimental investigation of the rheological behavior and viscosity of decorated multi-walled carbon nanotubes with TiO_2 nanoparticles/water nanofluids. J Therm Anal Calorim 123(1):81–9.

Bellos E, Tzivanidis CJD (2018) Thermal analysis of parabolic trough collector operating with mono and hybrid nanofluids. J Sustain Energy Technol Assess 26:105–15.

Bianco V, Chiacchio F, Manca O, Nardini S (2009) Numerical investigation ofnanofluids forced convection in circular tubes. Appl. Therm. Eng 29:3632-3642.

Bianco V, Manca O, Nardini S (2011) Numerical investigation on nanofluids turbulent convection heat transfer inside a circular tube, Int. J. Therm. Sci. 50: 341-349.

Bobbo S, Fedele L, Benetti A, Colla L, Fabrizio M, Pagura C, Barison S (2012) Viscosity of water based SWCNH and TiO_2nanofluids. Exp. Therm Fluid Sci. 36: 65–71.

Brinkman H. The viscosity of concentrated suspensions and solutions. J Chem Phys 1952:20(4):571.

Chakraborty S, Panigrahi PK (2020) Stability of nanofluid: A review, Appl. Therm. Eng. 115259.

Choi SU, J.A. Eastman JA (1995) Enhancing thermal conductivity of fluids with nanoparticles, Argonne National Lab, IL (United States).

Das SK, Putta N, Thiesen P, Roetzel W (2003) Temperature dependence of thermal conductivity enhancement for nanofluids. J. Heat Transfer 125: 567–574.

Duffie JA, Beckman WA (2013). Solar engineering of thermal processes solar engineering. John Wiley & Sons Inc.

Esfe MH, Saedodin S (2015) Turbulent forced convection heat transfer and thermophysical properties of MgO–water nanofluid with consideration of different nanoparticles diameter, an empirical study. J Therm Anal Calorim 119(2):1205–13.

Fedele L, Colla L, Bobbo S (2012) Viscosity andthermal conductivity measurements of water-based nanofluids containing titanium oxide nanoparticles. Int. J. Refrig. 35: 1359–1366.

Gupta M, Singh V, Said Z (2020) Heat transfer analysis using zinc Ferrite/water (Hybrid) nanofluids in a circular tube: An experimental investigation and development of new correlations for thermophysical and heat transfer properties. Sustain. Energy Technol. Assess 39: 100720.

Hamilton RL, Crosser O (1962) Thermal conductivity of heterogeneous two- component systems. Ind. Eng. Chem. Fundam 1 (3) :187–191.

He Y, Men Y, Zhao Y, Lu H, Ding Y (2009) Numerical investigation into theconvective heat transfer of TiO2nanofluids flowing through a straight tube under the laminar flow conditions. Appl. Therm. Eng 29 :1965-1972.

Khin N, Choudhury IA, Masjuki HH, Aoyama H (2017) Theoretical analysis to determine the efficiency of a CuO-water nanofluid based-flat plate solar collector for domestic solar water heating system in Myanmar. Sol. Energy 155: 608–619.

Labib MN, Nine MJ, Afrianto H, Chung H, Jeong H (2013) Numerical investigationon effect of base fluids and hybrid nanofluid in forced convective heat transfer, Int. J. Thermal Sci 71:163-171.

Lotfi R, Saboohi Y, Rashidi AM (2010) Numerical study of forced convective heat transfer of nanofluids: comparison of different approaches, Int. Comm. Heat Mass Trans 37:74-78.

Mahian O, Kianifar A, Sahin AZ, Wongwises S (2014) Entropy generation during Al_2O_3/water nanofluid flow in a solar collector: effects of tube roughness, nanoparticlesize, and different thermophysical models. Int J Heat Mass Transf 78:64–75.

Mahian O, Kianifar A, Sahin AZ, Wongwises S (2014) Performance analysis of a minichannel-based solar collector using different nanofluids. Energy Convers Manag 88:129–38.

Maiga SE, Palm SJ, Nguyen CT, Roy G, Galanis N (2005) Heat transfer enhancement by using nanofluids in forced convection flows. Int J Heat Fluid Flow. 1:26(4):530-46.

Maxwell JC. A treatise on electricity and magnetism.Oxford:Clarendon Press; 1873.

Minea AA (2017) Challenges in hybrid nanofluids behavior in turbulent flow: recent research and numerical comparison. J Renew Sustain Energy Rev 71:426–34.

Murshed SMS, Leong KC, Yang C (2005) Enhanced thermal conductivity of TiO_2—water based nanofluids. Int. J. Therm. Sci. 44 (4): 367–373.

Mwesigye A, Huan Z (2015) Thermal and thermodynamic performance of a parabolic trough receiver with Syltherm800-Al_2O_3nanofluidas the heat transfer fluid. J Energy Procedia 75:394–402.

514 Okonkwo EC, Abid M, Ratlamwala TAH (2019) Comparative study of heat transfer
515 enhancement in parabolic trough collector based on modified absorber geometry. EnergyEng
516 ASCE 145(3):1−16.

517 Okonkwo EC, Abid M, Ratlamwala TAH, Abbasoglu S, Dagbasi M (2019) Optimal analysis
518 of entropy generation and heat transfer in parabolic trough collector using green synthesized
519 TiO_2/water nanofluids. J Sol Energy Eng 141(3):310111.

520 Okonkwo EC, Ratlamwala TAH, Abid M (2019) Energy, exergy, exergoeconomic, and
521 exergoenvironmental study of a parabolic trough collector using a converging-diverging
522 receiver tube. International Journal of Exergy 29(2-4):131-154..

523 Otanicar T, Phelan PE, Prasher RS, Rosengarten G, Taylor RA (2010) Nanofluid based direct
524 absorption solar collector, J. Renew. Sust.Energy 2:033102.

525 Ozil E, Yaşar K (1987) Analysis of flat plate collectors. In: Yuncu, H., Paykoc,E., Yener, Y.
526 (Eds.) Solar Energy Utilization. Springer Dordrecht 188−213.

527 Padilla RV, Fontalvo A, Demirkaya G, Martinez A, Quiroga AG (2014) Exergy analysis of
528 parabolic trough solar receiver. Appl Therm Eng 67(1−2):579−86.

529 Pak BC., Cho YI (1998) Hydrodynamic and heat transfer study of dispersed fluids with
530 submicron metallic oxide particles. Exp. Heat Transfer 11: 151–170.

531 Petela R (1964) Exergy of heat radiation. J Heat Transfer 86(2):187.

532 Prakasam MJS, ThottipalayamVellingiri A, Nataraj S (2017) An experimental study of the
533 mass flow rates effect on flat-plate solar water heater performance using Al_2O_3/water
534 nanofluid.Therm Sci 21:S379–88.

535 Rasih RA, Sidik NAC, Samion S (2019) Recent progress on concentrating direct absorption
536 solar collector using nanofluids. JTherm Anal Calorim 137:903–22.

537 Said Z, Saidur R, Rahim NA (2014) Optical properties of metal oxides based nanofluids. Int.
538 Commun. Heat Mass Transfer 59: 46–54.

Sajid MH, Said Z, Saidur R, Adikan FRM, Sabri MFM, Rahim NA (2014) A time variant investigation on optical properties of water based Al_2O_3nanofluid. Int. Commun. Heat Mass Transfer 50: 108–116.

Sarkar J, Ghosh P, Adil A (2015) A review on hybrid nanofluids: recent research, development and applications. Renew. Sustain. Energy Rev. 43: 164–177.

Sundar LS, Sharma K, Singh MK, Sousa A (2017) Hybrid nanofluids preparation, thermal properties, heat transfer and friction factor–a review. Renew Sustain Energy Rev 68:185–98.

Suresh S, Venkitaraj KP, Selvakumar P, Chandrasekar M (2011) Synthesis of Al_2O_3–Cu/water hybrid nanofluids using two step method and its thermo physical properties. Colloids Surf A 388 (1–3): 41–48.

Takabi B, Salehi S (2014) Augmentation of the heat transfer performance of a sinusoidal corrugated enclosure by employing hybrid nanofluid. JAdvMech Eng 6:147059.

Tyagi H, Phelan P, Prasher R (2009) Predicted efficiency of a low-temperature nanofluid 581 based direct absorption solar collector, J. Sol. Energy. Eng 13:041004–1.

Vajjha RS, Das DK, Mahagaonkar BM (2009) Density measurement of different nanofluids and their comparison with theory. Pet. Sci. Technol. 27 (6): 612–624.

Acknowledgements

Authors would like to express their deep gratitude to Audisankara College Engineering &Technology, Gudur to provide research facilities for carry out this research work

Availability of data and materials

Data will be made available upon request

Authors' contributions

P. Michael Joseph Stalin: Conceptualization, Methodology, Writing - original draft.

T.V. Arjunan: Validation. and Supervision.

Mohammed Almeshaal: Formal analysis, Investigation,

Murugesan Palaniappan: Writing - review & editing.

B.Prabu: Visualization.

P. Manoj Kumar: Validation,

Declarations

Ethics approval and consent to participate Not applicable

Consent to publish

Not applicable

Competing interests

The authors declare no competing interests

Funding

Not applicable